Inorg. Chem. **2007**, *46*, 2716–2724

Inorganic Chemistry
Article

Synthesis, Structure, Reactivity, and Thermal Isomerization of Boron-Substituted 13-Vertex Cobaltacarboranes (η^5-Cp)Co(η^6-$R_2C_2B_{10}Me_8H_2$) (R = H, Et)

Liang Deng, Hoi-Shan Chan, and Zuowei Xie*

Department of Chemistry and Center of Novel Functional Molecules, The Chinese University of Hong Kong, Shatin, New Territories, Hong Kong, China

Received December 18, 2006

Reduction of boron-substituted carboranes *o*-$R_2C_2B_{10}Me_8H_2$ (R = H, Et), thermal isomerization, and nucleophilic reaction of the resultant 13-vertex cobaltacarboranes were studied. Reaction of *o*-$C_2B_{10}Me_8H_4$ (**1**) with excess potassium metal in tetrahydrofuran (THF) gave, after recrystallization from a THF solution of 18-crown-6 ether, {[K(18-crown-6)$(THF)_2$][K(18-crown-6)]}{[4-(18-crown-6)-2,3,5,8,9,11,12,13-Me_8-4,1,6-$KC_2B_{10}H_4]_2$} (**2**) in 78% yield. Interaction of **1** with excess sodium or potassium metal in THF, followed by treatment with $CoCl_2$/CpNa and then aerobatic oxidation, afforded two boron-substituted 13-vertex cobaltacarboranes, 4-Cp-2,3,5,8,9,11,12,13-Me_8-4,1,6-$CoC_2B_{10}Me_8H_4$ (**3**) and 4-Cp-2,3,5,9,10,11,12,13-Me_8-4,1,6-$CoC_2B_{10}Me_8H_4$ (**4**), in 15% and 8% yield, respectively. Subsequently, thermal isomerization of **3** and **4** yielded another two new isomers, 4-Cp-2,3,5,6,8,11,12,13-Me_8-4,1,9-$CoC_2B_{10}Me_8H_4$ (**5**) and 4-Cp-2,3,5,6,7,11,12,13-Me_8-4,1,9-$CoC_2B_{10}Me_8H_4$ (**6**). Treatment of **3** or **4** with strong bases such as ^{n}BuLi and MeLi generated unexpected nucleophilic substitution products 4-^{n}BuCp-2,3,5,8,9,11,12,13-Me_8-4,1,6-$CoC_2B_{10}Me_8H_4$ (**7**), 4-^{n}BuCp-2,3,5,9,10,11,12,13-Me_8-4,1,6-$CoC_2B_{10}Me_8H_4$ (**8a**), and 4-MeCp-2,3,5,9,10,11,12,13-Me_8-4,1,6-$CoC_2B_{10}Me_8H_4$ (**8b**) in good yields. Under the same reaction conditions, however, only one 13-vertex cobaltacarborane, 4-Cp-1,9-Et_2-2,5,6,7,8,11,12,13-Me_8-4,1,9-$CoC_2B_{10}Me_8H_4$ (**10**), was isolated when *o*-$Et_2C_2B_{10}Me_8H_2$ (**9**) was used as the starting material. Complex **10** is a thermodynamically stable product and has a substitution pattern different from that of **3**–**6**. These results show that the substituents on either the cage carbon or boron atoms have an important effect on the formation and thermal stability of the 13-vertex metallacarboranes. The formation of these complexes can be rationalized by the diamond–square–diamond mechanism.

Introduction

Polyhedral rearrangement is a well-known property of carboranes and metallacarboranes.[1] Many attempts have been made to determine the mechanisms of this complicated process. Accordingly, several isomerization pathways have been proposed on the basis of thermal isomerization of icosahedral carboranes.[2] In contrast, the studies on docosahedral molecules are largely unexplored and have limited migration of carbon vertices,[3] which have revealed that thermal isomerization always leads to the separation of the cage carbon atoms.[3] For example, transformation from the 4,1,6 to 4,1,9 (4,1,8-) to 4,1,12 isomer of (η^5-Cp)Co(η^6-$C_2B_{10}H_{12}$) can be successively achieved upon heating (Chart 1 shows the numbering system of a docosahedron).[3a] Obviously, the simultaneous movement of boron vertices is inevitable during the process. This issue has not been addressed in docosahedral molecules probably because of the complexity of the movement of boron vertices caused

---

* To whom correspondence should be addressed. E-mail: zxie@cuhk.edu.hk. Tel: (852)26096269. Fax: (852)26035057.

(1) (a) Onak, T. Polyhedral Carbaboranes. In *Comprehensive Organometallic Chemistry II*; Abel, E. W., Stone, F. G. A., Wilkinson, G., Eds.; Pergamon: New York, 1995; Vol. 1, p 217. (b) Grimes, R. N. Metallacarboranes. In *Comprehensive Organometallic Chemistry II*; Abel, E. W., Stone, F. G. A., Wilkinson, G., Eds.; Pergamon: New York, 1995; Vol. 1, p 373.

(2) (a) Hoffmann, R.; Lipscomb, W. N. *Inorg. Chem.* **1963**, *1*, 231. (b) Fein, M.; Bobinski, J.; Mayes, N.; Schwartz, N.; Cohen, M. S. *Inorg. Chem.* **1963**, *2*, 1111. (c) Kaesz, H. D.; Bau, R.; Beall, H. A.; Lipscomb, W. N. *J. Am. Chem. Soc.* **1967**, *89*, 4218. (d) Hart, H. V.; Lipscomb, W. N. *J. Am. Chem. Soc.* **1969**, *91*, 771. (e) Grafstein, D.; Dvorak, J. *Inorg. Chem.* **1963**, *2*, 1123. (f) Zakharkin, L. I.; Kalinin, V. N. *Dokl. Akad. Nauk SSSR* **1966**, 169. (g) Muetterties, E. L.; Knoth, W. H. *Polyhedra Boranes*; Marcel Dekker: New York, 1968; p 55. (h) Lipscomb, W. N. *Science* **1966**, *153*, 373. (i) Wong, H. S.; Lipscomb, W. N. *Inorg. Chem.* **1975**, *14*, 1350. (j) Wu, S. H.; Jones, M., Jr. *J. Am. Chem. Soc.* **1989**, *111*, 5373. (k) Edvenson, G. M.; Gaines, D. F. *Inorg. Chem.* **1990**, *29*, 1210.

10.1021/ic062423t CCC: $37.00

Chart 1. Numbering Diagram of Docosahedron

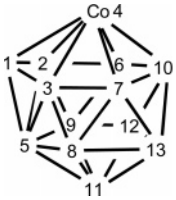

Scheme 1

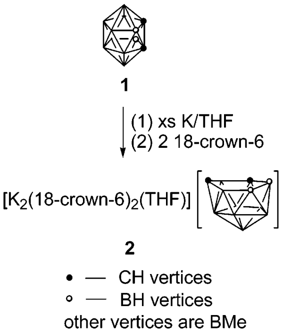

by a large number of boron atoms. On the other hand, it is well documented that reduction of *o*-$R_2C_2B_{10}H_{10}$ with group 1 metals results in the formation of [*nido*-$R_2C_2B_{10}H_{10}]^{2-}$, in which the two carbon vertices are always on the C_2B_4 open face regardless of the substituents on the cage carbons.[4] However, the parallel study on cage boron vertices has not yet appeared in the literature. If some boron atoms of the cage can be distinguished from the others, such a carborane may offer useful information on the migration of cage boron vertices during the isomerization process. With this in mind, 4,5,7,8,9,10,11,12-Me_8-1,2-R_2-1,2-$C_2B_{10}H_2$ (R = H, Et) were chosen as model compounds for this purpose[5] because the two BH vertices can be easily discriminated from the other BMe ones. Herein, we report our work on the reduction of these two carboranes with group 1 metals, and the synthesis, structure, and thermal isomerization of the resultant 13-vertex metallacarboranes (η^5-Cp)Co(η^6-$R_2C_2B_{10}Me_8H_2$) (R = H, Et), as well as their reactivities toward nucleophiles.

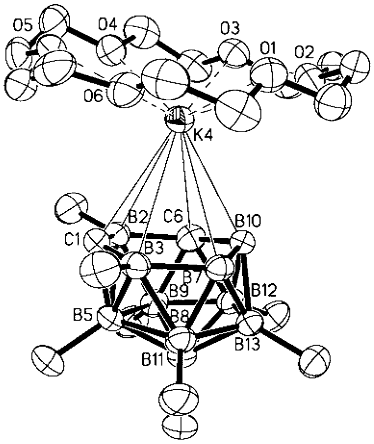

Figure 1. Structure of [4-(18-crown-6)-2,3,5,8,9,11,12,13-Me_8-4,1,6-$KC_2B_{10}H_4]^-$ in **2**.

Scheme 2

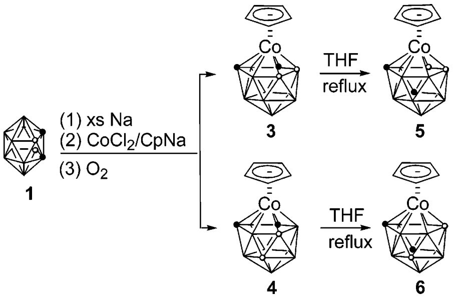

Results and Discussion

Reduction of 4,5,7,8,9,10,11,12-Me_8-1,2-$C_2B_{10}H_4$ (1) with Group 1 Metals. Treatment of **1** with excess potassium or sodium metal in tetrahydrofuran (THF) at room temperature gave presumably [*nido*-$C_2B_{10}Me_8H_4$][M$(THF)_x]_2$ (M = Na, K) with identical ^{11}B NMR spectra, which suggests that the same *nido*-carborane dianion was generated. Recrystallization of the potassium salt from a THF solution of 18-crown-6 ether afforded {[K(18-crown-6)$(THF)_2$][K(18-crown-6)]}{[4-(18-crown-6)-2,3,5,8,9,11,12,13-Me_8-4,1,6-$KC_2B_{10}H_4]_2$} (**2**) as colorless crystals in 78% yield (Scheme 1). Complex **2** was characterized by various spectroscopic techniques and elemental analyses. Its ^1H NMR spectrum showed a molar ratio of two 18-crown-6 and one THF molecules per carborane cage. The $^{11}B\{^1H\}$ NMR spectrum displayed 10 distinct peaks in the range +21.3 to −19.5 ppm. Many attempts to grow single crystals of the corresponding sodium salt failed.

Single-crystal X-ray analyses revealed that **2** is an ionic salt consisting of well-separated, alternating layers of discrete ions [K(18-crown-6)$(THF)_2]^+$, [K(18-crown-6)$]^+$, and [4-(18-crown-6)-2,3,5,8,9,11,12,13-Me_8-4,1,6-$KC_2B_{10}H_4]^-$. In the anion, the potassium atom occupies the 4 position to form a 13-vertex potassacarborane (Figure 1). The average K4−cage atom distance of 3.233(5) Å is close to the corresponding value of 3.174(2) Å observed in [{$(C_6H_5CH_2)_2C_2B_{10}H_{10}$}-$K_2(THF)_2(O_2C_4H_8)_{0.5}]_n$.[4f] Similar to other carbon-atoms-apart *nido*-carborane anions,[4f,g] the six atoms of the open hexagonal C_2B_4 bonding face in **2** are almost coplanar with the two CH vertices occupying the 1 and 6 positions, respectively. The C1 atom is less coordinated, resulting in shorter C1−B distances with an average value of 1.584(8) Å (Table 1).

To the best of our knowledge, there is no report on the reduction of boron-substituted *o*-carboranes. Therefore, it is

---

(3) (a) Dunks, G. B.; McKown, M. M.; Hawthorne, M. F. *J. Am. Chem. Soc.* **1971**, *93*, 2541. (b) Dustin, D. F.; Dunks, G. B.; Hawthorne, M. F. *J. Am. Chem. Soc.* **1973**, *95*, 1109. (c) Salentine, C. G.; Hawthorne, M. F. *J. Am. Chem. Soc.* **1975**, *97*, 426. (d) Salentine, C. G.; Hawthorne, M. F. *Inorg. Chem.* **1976**, *15*, 2872. (e) Burke, A.; McIntosh, R.; Ellis, D.; Rosair, G. M.; Welch, A. J. *Collect. Czech., Chem. Commun.* **2002**, *67*, 991. (f) Ellis, D.; Lopez, M. E.; McIntosh, R.; Rosair, G. M.; Welch, A. J.; Quenardelle, R. *Chem. Commun.* **2005**, 1348.

(4) (a) Fein, M.; Bobinski, J.; Mayes, N.; Schwartz, N.; Cohen, M. S. *Inorg. Chem.* **1963**, *2*, 1111. (b) Grafstein, D.; Dvorak, J. *Inorg. Chem.* **1963**, *2*, 1128. (c) Dunks, G. B.; Wiersema, R. J.; Hawthorne, M. F. *J. Am. Chem. Soc.* **1973**, *95*, 3174. (d) Tolpin, E. I.; Lipscomb, W. N. *Inorg. Chem.* **1973**, *12*, 2257. (e) Churchill, M. R.; DeBoer, B. G. *Inorg. Chem.* **1973**, *12*, 2674. (f) Chui, K.; Li, H.-W.; Xie, Z. *Organometallics* **2000**, *19*, 5447. (g) Zi, G.; Li, H.-W.; Xie, Z. *Organometallics* **2001**, *20*, 3836. (h) Zi, G.; Li, H.-W.; Xie, Z. *Chem. Commun.* **2001**, 1110. (i) Zi, G.; Li, H.-W.; Xie, Z. *Organometallics* **2002**, *21*, 5415. (j) Deng, L.; Cheung, M.-S.; Chan, H.-S.; Xie, Z. *Organometallics* **2005**, *24*, 6244. (k) Shen, H.; Chan, H.-S.; Xie, Z. *Organometallics* **2006**, *25*, 2617.

(5) Herzog, A.; Knobler, C.; Hawthorne, M. F.; Maderna, A.; Siebert, W. *J. Org. Chem.* **1999**, *64*, 1045.

Table 1. Selected Distances (Å) in 13-Vertex Cobaltacarboranes[a]

	2	**3**	**4**	**5**	**6**	**7**	**8a**	**8b**	**10**	**A**[b]	**A***[c]	**B***[c]
Co−Cent(Cp)		1.67	1.68	1.68	1.67	1.67	1.67	1.68	1.68	1.65	1.69	1.69
Co−Cent(Carb)		1.36	1.35	1.31	1.33	1.36	1.35	1.35	1.32	1.34	1.35	1.32
av C1−B	1.584(8)	1.602(3)	1.601(4)	1.60(1)	1.61(1)	1.56(1)	1.600(8)	1.598(4)	1.59(1)	1.577(6)	1.600(4)	1.561(5)
av C6/C9−B	1.684(8)	1.707(4)	1.696(5)	1.73(1)	1.77(1)	1.72(1)	1.696(9)	1.739(5)	1.75(1)	1.688(7)	1.694(4)	1.748(5)
av B−Me	1.616(8)	1.599(4)	1.598(5)	1.59(1)	1.59(1)	1.60(1)	1.595(9)	1.589(8)	1.61(1)			
B2−B5	2.033(9)	2.098(4)	2.059(6)	2.00(1)	2.01(1)	2.11(1)	2.125(9)	2.071(5)	1.98(1)	1.948(7)	1.985(4)	1.967(5)
B3−B5	2.093(9)	2.045(4)	2.058(6)	2.01(1)	2.01(1)	2.02(1)	2.005(8)	2.071(5)	2.01(1)	2.081(7)	2.089(4)	2.015(5)

[a] Cent(Cp) or Cent(Carb): the centroid of the Cp ring or the C_2B_4 bonding face. [b] **A** = 4-Cp-4,1,6-$CoC_2B_{10}H_{12}$; see ref 6. [c] **A*** = 4-Cp*-4,1,6-$CoC_2B_{10}H_{12}$; **B*** = 4-Cp*-4,1,9-$CoC_2B_{10}H_{12}$; see ref 3e.

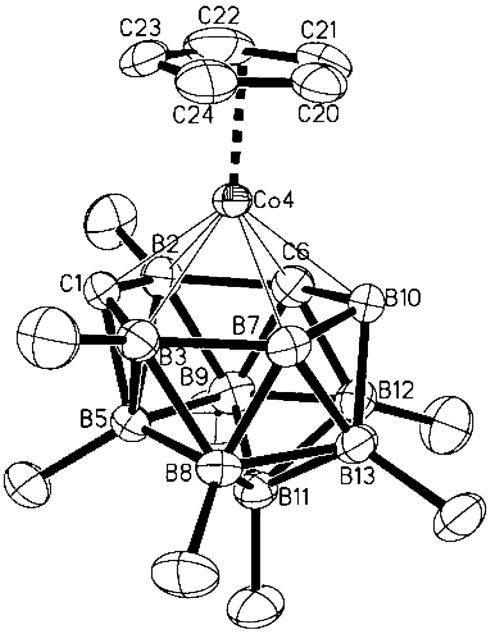

Figure 2. Molecular structure of **3**.

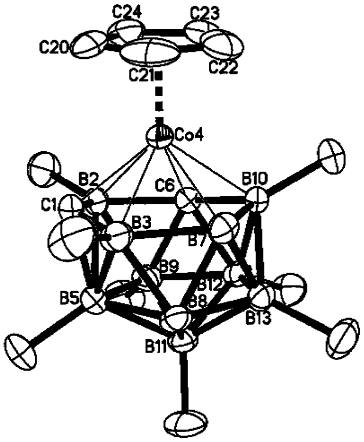

Figure 3. Molecular structure of **4**.

interesting to know where the two BH vertices are located after the reduction. As shown in Figure 1, the two BH vertices in **2** are on the open hexagonal C_2B_4 bonding face together with the two CH ones. The ^{11}B NMR experiments indicated that **2** can be converted into a mixture of isomers upon heating, which suggests that it should be a kinetic product. Attempts to isolate a pure isomer from the mixture were unsuccessful.

Synthesis, Structure, and Thermal Isomerization of 13-Vertex Cobaltacarboranes ($(\eta^5$-Cp)Co(η^6-$C_2B_{10}Me_8H_4$)). Similar to the procedures described for the preparation of (η^5-Cp)Co(η^6-$C_2B_{10}H_{12}$),[3a] reduction of **1** with sodium or potassium metal in THF followed by treatment with $CoCl_2$/NaCp gave, after aerobic oxidation and column separation, two 13-vertex cobaltacarboranes, 4-Cp-2,3,5,8,9,11,12,13-Me_8-4,1,6-$CoC_2B_{10}Me_8H_4$ (**3**) and 4-Cp-2,3,5,9,10,11,12,13-Me_8-4,1,6-$CoC_2B_{10}Me_8H_4$ (**4**), regardless of the group 1 metal used in ca. 15% and 8% yield, respectively, both as deep-red crystals (Scheme 2). Complexes **3** and **4** were quantitatively (by ^{11}B NMR) converted to their structural isomers 4-Cp-2,3,5,6,8,11,12,13-Me_8-4,1,9-$CoC_2B_{10}Me_8H_4$ (**5**) and 4-Cp-2,3,5,6,7,11,12,13-Me_8-4,1,9-$CoC_2B_{10}Me_8H_4$ (**6**) upon refluxing of their THF solutions overnight. The interconversion between **3** and **4** was not observed in the temperature range 25−60 °C, as indicated by ^{11}B NMR. Complexes **5** and **6** underwent further thermal isomerization in refluxing toluene, affording a mixture of inseparable products with very complicated ^1H and ^{11}B NMR spectra.

Complexes **3**−**6** are air- and moisture-stable and soluble in common organic solvents such as toluene, CH_2Cl_2, and THF. They were characterized by various NMR techniques and single-crystal X-ray analyses. Their ^1H NMR spectra displayed a sharp singlet of area 5 at ~ 5.2 ppm assignable to the cyclopentadienyl protons, two broad singlets of area 2 corresponding to the two cage CH protons (at 4.14 and 3.03 ppm for **3**, 3.88 and 3.17 ppm for **4**, 3.54 and 1.53 ppm for **5**, and 3.61 and 1.44 ppm for **6**), and a set of singlets of total area 24 between +1.0 and −0.5 ppm attributable to BMe protons. The ^{11}B NMR spectra showed a 1:1:1:2:2:1:1:1 pattern in the range +15.6 to −6.2 ppm for **3**, a 2:1:2:1:1:1:1:1 pattern in the range +13.0 to −8.3 ppm for **4**, a 1:1:1:1:1:1:2:1:1 pattern in the range +23.2 to −4.7 ppm for **5**, and a 1:1:1:1:2:3:1 pattern in the range +28.6 to −9.9 ppm for **6**.

Single-crystal X-ray analyses revealed that **3**−**6** adopt a docosahedral geometry, with the cobalt atom occupying the 4 position and the two CH and two BH vertices being located at the 1, 6, 7, and 10 positions in **3**, 1, 6, 7, and 8 positions in **4**, 1, 9, 7, and 10 positions in **5**, and 1, 9, 8, and 10 positions in **6**, shown in Figures 2−5, respectively. The Co4−Cent(Cp) and Co4−Cent(Carb) distances in **3**−**6** are very close to each other and are similar to those observed in 4-Cp-4,1,6-$CoC_2B_{10}H_{12}$ (**A**),[6] 4-Cp*-4,1,6-$CoC_2B_{10}H_{12}$ (**A***),[3e] and 4-Cp*-4,1,9-$CoC_2B_{10}H_{12}$ (**B***)[3e] (Table 1). The average distances of C1 to its neighboring atoms are 1.602(3) Å in **3**, 1.601(4) Å in **4**, 1.60(1) Å in **5**, and 1.61(1) Å in **6**, which are shorter than the corresponding values observed for the

---

(6) Churchill, M. R.; DeBoer, B. G. *Chem. Commun.* **1972**, 1326.

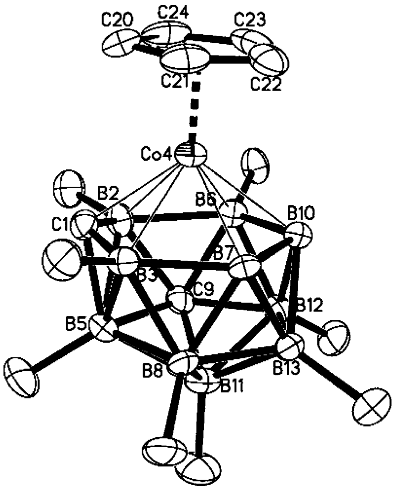

Figure 4. Molecular structure of **5**.

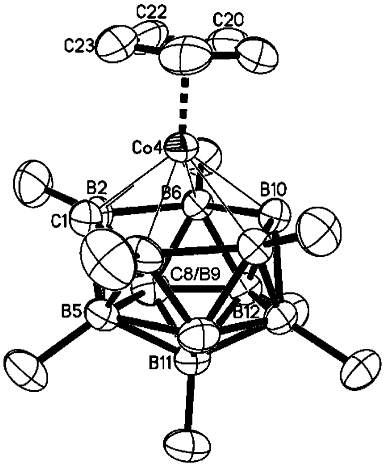

Figure 5. Molecular structure of **6** (note that the C8 and B9 atoms of the cage are indistinguishable because of the presence of a crystallographic mirror plane through Co4, C1, and B10 atoms).

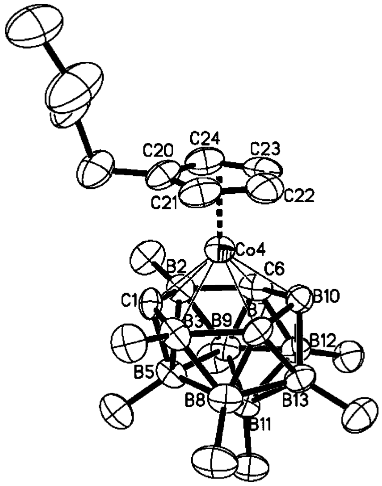

Figure 6. Molecular structure of **7**.

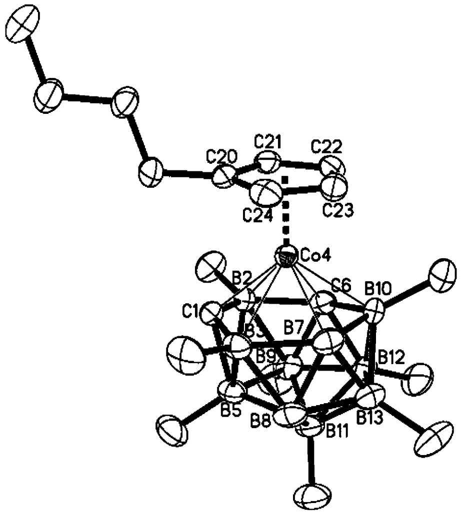

Figure 7. Molecular structure of **8a**.

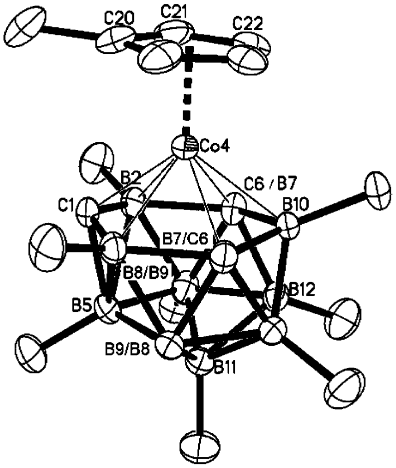

Figure 8. Molecular structure of **8b** (note that the C6/B7 and B8/B9 atoms of the cage are indistinguishable because of the presence of a crystallographic mirror plane through Co4, C1, and B10 atoms).

second cage carbon, 1.707(4) Å in **3**, 1.696(5) Å in **4**, 1.73(1) Å in **5**, and 1.77(1) Å in **6**. These results may be ascribed to the different coordination numbers of the two cage carbons. Similar phenomena are also observed in **A**, **A***, and **B***.[3e,6] The average B−Me distance of ~1.60 Å in **3**−**6** is very comparable to that of 1.587(9) Å in 8,9,10,11,12,13-$(CH_3)_6$-1,2-$(CH_2)_3$-1,2-$C_2B_{11}H_5$[7] and 1.58(1) Å in 4,5,7,8,9,10,11,12-$(CH_3)_8$-1,2-$C_2B_{10}H_4$.[5] In view of the ^1H NMR chemical shifts of the cage CH vertices and the crystal structures of **3**−**6**, a high-field chemical shift of the cage CH proton is observed when the CH vertex migrates from the hexagonal belt to the pentagonal one. Such a trend is also found in the ^1H NMR spectra of $(\eta^5\text{-Cp})Co(\eta^5\text{-}C_2B_{10}H_{12})$[3b] and $(\eta^5\text{-Cp*})Co(\eta^5\text{-}C_2B_{10}H_{12})$.[3e] Therefore, the chemical shifts of the cage CH protons may serve as indicators to locate the relative positions of the cage carbons.

Comparison among the crystal structures of **2**−**4** suggests that **3** should result from the direct capitation of **2**, whereas a coincident isomerization, rather than a sequential isomerization of **3**, may be involved in the capitation reaction to yield **4**.[8] This argument is supported by various temperature ^{11}B NMR experiments, which indicate the absence of interconversion between **3** and **4**. The formation of **5** and **6** from **3** and **4**, respectively, can be rationalized by the diamond−square−diamond (DSD) mechanism (vide infra).[2h] Although the movement of cage CH vertex from the 6

---

[7] Deng, L.; Chan, H.-S.; Xie, Z. *J. Am. Chem. Soc.* **2006**, *128*, 5218.

Scheme 3

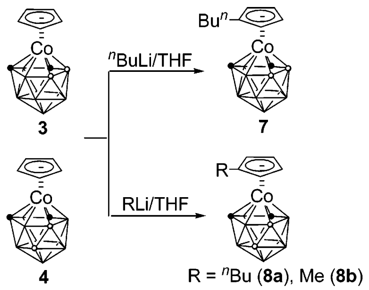

Scheme 4

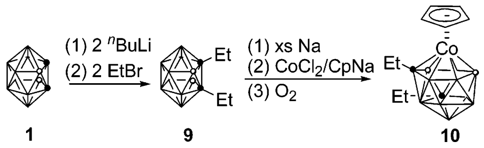

Scheme 5

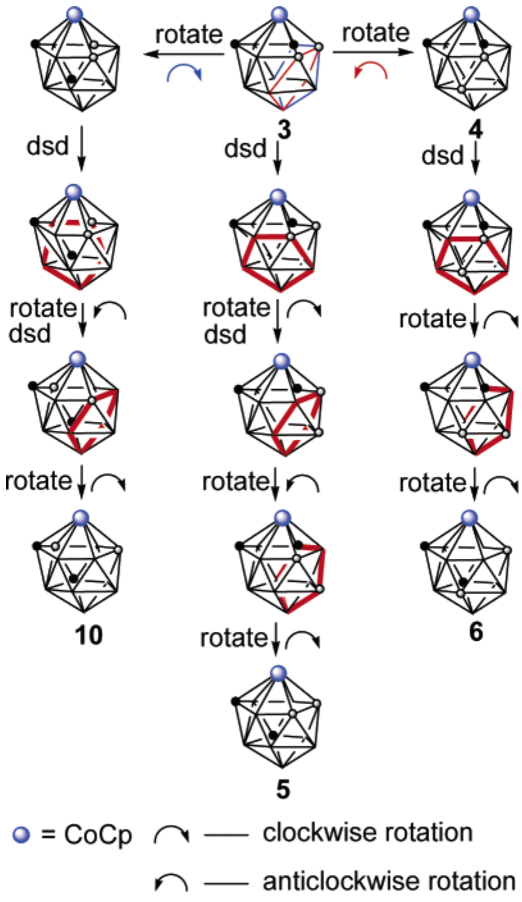

position to the 9 position is a well-documented phenomenon for 13-vertex metallacarboranes,[3] the well-regulated migration of BH vertices from the 7 and 8 positions to the 8 and 10 positions in the conversion of **4** to **6** is observed for the first time. To our surprise, the above isomerization in THF gives only one product though several possible isomers were anticipated. It is suggested that the substituents on the cage play a role in this process.

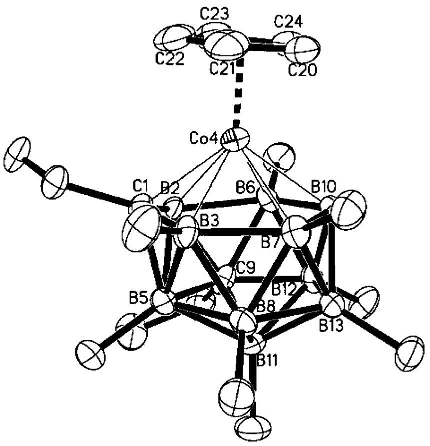

Figure 9. Molecular structure of **10**.

Nucleophilic Substitution Reaction of 13-Vertex Cobaltacarboranes. Considering the acidity of the cage CH proton, we attempted to convert the CH vertices to CR ones using the lithiation/alkylation approach.[9] Treatment of **3** with 1 or 2 equiv of ^{n}BuLi in THF followed by the addition of MeI gave, after column chromatographic separation, 4-^{n}-BuCp-2,3,5,8,9,11,12,13-Me$_8$-4,1,6-CoC$_2$B$_{10}$Me$_8$H$_4$ (**7**) in 82% yield. Because no methylation product was observed in this reaction, **7** should result from the direct nucleophilic substitution reaction of the Cp ring. Similarly, interaction of **4** with ^{n}BuLi or MeLi also generated the Cp-ring-substituted products 4-^{n}BuCp-2,3,5,9,10,11,12,13-Me$_8$-4,1,6-CoC$_2$B$_{10}$Me$_8$H$_4$ (**8a**) or 4-MeCp-2,3,5,9,10,11,12,13-Me$_8$-4,1,6-CoC$_2$B$_{10}$Me$_8$H$_4$ (**8b**) in 81% or 85% yield, respectively (Scheme 3). It is noteworthy that such a nucleophilic substitution reaction did not proceed when LiNEt$_2$ and KOBu^t were used as nucleophilies.

Complexes **7**, **8a**, and **8b** were fully characterized by various spectroscopic techniques and single-crystal X-ray analyses. Their ^{11}B NMR spectra are similar to those of the parent molecules, exhibiting a 1:1:1:2:2:2:1 pattern in the range +15.4 to −6.6 ppm for **7**, a 2:1:2:1:1:1:1:1 pattern in the range +13.5 to −7.0 ppm for **8a**, and a 2:1:2:1:1:1:1:1 pattern in the range +12.0 to −8.5 ppm for **8b**. As shown in Figures 6−8, single-crystal X-ray analyses revealed that the ^{n}Bu and Me groups are directly bonded to the Cp ring and the cage geometries are almost identical with their parent complexes **3** and **4**. For comparison, the selected structural parameters are compiled in Table 1.

This type of nucleophilic substitution reaction has been observed in some cationic metallocenes of late transition metals[10] and the mixed metallacarborane CpCo(η^5-Et$_2$C$_2$B$_4$H$_4$).[11] For example, both (^{n}BuC$_5$H$_4$)Co(η^5-Et$_2$C$_2$B$_4$H$_4$)

---

(8) The coincident formation of several isomers of a metallacarborane in the metallation step has been well-documented. For recent examples, see: (a) Grüner, B.; Štíbr, B.; Kivekäs, R.; Sillanpää, R.; Stopka, P.; Teixidor, F.; Viñas, C. *Chem.—Eur. J.* **2003**, *9*, 6115. (b) Perekalin, D. S.; Glukhov, I. V.; Štíbr, B.; Kudinov, A. R. *Inorg. Chim. Acta* **2006**, *359*, 3264. (c) McIntosh, R. D.; Ellis, D.; Giles, B. T.; Macgregor, S. A.; Rosair, G. M.; Welch, A. J. *Inorg. Chim. Acta* **2006**, *359*, 3745.

(9) Rees, W. S., Jr.; Schubert, D. M.; Knobler, C. B.; Hawthorne, M. F. *J. Am. Chem. Soc.* **1986**, *108*, 5369.

(10) (a) Forschner, T. C.; Cooper, N. J. *J. Am. Chem. Soc.* **1989**, *111*, 7420. (b) Kirchner, K.; Taube, H. *J. Am. Chem. Soc.* **1991**, *113*, 7039. (c) Comte, V.; Blacque, O.; Kubicki, M. M.; Moise, C. *Organometallics* **2001**, *20*, 5432. (d) Tane, J. P.; Vollhardt, K. P. C. *Angew. Chem., Int. Ed. Engl.* **1982**, *21*, 617.

Table 2. Crystal Data and Summary of Data Collection and Refinement for **2**−**6**

	2	**3**	**4**	**5**	**6**
formula	$C_{38}H_{84}B_{10}K_2O_{13}$	$C_{15}H_{33}B_{10}Co$	$C_{15}H_{33}B_{10}Co$	$C_{15}H_{33}B_{10}Co$	$C_{15}H_{33}B_{10}Co$
cryst size, mm	0.40 × 0.25 × 0.20	0.40 × 0.30 × 0.20	0.40 × 0.30 × 0.20	0.40 × 0.30 × 0.20	0.20 × 0.15 × 0.10
fw	935.40	380.44	380.44	380.44	380.44
cryst syst	triclinic	monoclinic	monoclinic	orthorhombic	orthorhombic
space group	*P*(−1)	*P*2₁/*c*	*P*2₁/*n*	*Pbca*	*Pnma*
a, Å	11.921(2)	13.626(1)	10.063(3)	14.547(3)	14.150(3)
b, Å	12.162(2)	9.918(1)	16.035(5)	15.511(3)	13.758(3)
c, Å	20.104(4)	16.064(1)	13.155(4)	18.591(4)	10.681(2)
α, deg	75.28(3)	90	90	90	90
β, deg	73.23(3)	99.94(1)	97.66(1)	90	90
γ, deg	81.22(3)	90	90	90	90
V, Å^3	2698.3(9)	2138.3(2)	2104(1)	4195(1)	2079.3(7)
Z	2	4	4	8	4
D_{calcd}, Mg/m^3	1.155	1.182	1.201	1.205	1.215
radiation (λ), Å	Mo Kα (0.710 73)	Mo Kα (0.710 73)	Mo Kα (0.710 73)	Mo Kα (0.710 73)	Mo Kα (0.710 73)
2θ range, deg	2.2−50.0	3.0−50.0	4.0−56.0	4.4−50.0	4.8−48.0
μ, mm^{-1}	0.229	0.799	0.812	0.814	0.821
F(000)	1008	800	800	1600	800
no. of obsd reflns	5435	11108	14080	3679	4355
no. of params refnd	571	235	235	235	130
GOF	1.081	1.057	1.003	0.975	1.264
R1	0.067	0.041	0.050	0.058	0.084
*w*R2	0.178	0.117	0.123	0.135	0.158

Table 3. Crystal Data and Summary of Data Collection and Refinement for **7**, **8a**, **8b**, and **10**

	7	**8a**	**8b**	**10**
formula	$C_{19}H_{41}B_{10}Co$	$C_{19}H_{41}B_{10}Co$	$C_{16}H_{35}B_{10}Co$	$C_{19}H_{41}B_{10}Co$
cryst size, mm	0.30 × 0.25 × 0.20	0.25 × 0.20 × 0.10	0.50 × 0.40 × 0.30	0.43 × 0.27 × 0.19
fw	436.55	436.55	394.47	436.55
cryst syst	monoclinic	monoclinic	orthorhombic	monoclinic
space group	*P*2₁/*c*	*P*2₁/*c*	*Pnma*	*P*2₁/*c*
a, Å	9.014(2)	13.314(3)	17.509(1)	16.274(2)
b, Å	10.273(2)	10.011(2)	12.516(1)	9.967(1)
c, Å	27.164(5)	19.776(4)	10.073(1)	15.834(2)
β, deg	94.87(3)	106.67(3)	90	110.63(1)
V, Å^3	2506.4(9)	2525.2(9)	2207.4(2)	2403.6(4)
Z	4	4	4	4
D_{calcd}, Mg/m^3	1.157	1.148	1.187	1.206
radiation (λ), Å	Mo Kα (0.710 73)	Mo Kα (0.710 73)	Mo Kα (0.710 73)	Mo Kα (0.710 73)
2θ range, deg	4.2−48.0	4.3−40.0	4.6−50.0	2.7−50.0
μ, mm^{-1}	0.689	0.684	0.776	0.719
F(000)	928	928	832	928
no. of obsd reflns	4190	2106	11260	12880
no. of params refnd	271	271	141	271
GOF	0.978	1.049	1.134	0.922
R1	0.079	0.044	0.046	0.069
*w*R2	0.206	0.118	0.134	0.162

and $(IC_5H_4)Co(\eta^5\text{-}Et_2C_2B_4H_4)$ were isolated in 9% and 64% yield from the reaction of $CpCo(\eta^5\text{-}Et_2C_2B_4H_4)$ with ^{n}BuLi followed by treatment with I_2 in THF.[11] The isolation of **7**, **8a**, and **8b** in more than 80% yield suggests that the Cp rings of **3** and **4** are much better electrophiles than that of $CpCo(\eta^5\text{-}Et_2C_2B_4H_4)$. In other words, $[\eta^6\text{-}C_2B_{10}Me_8H_4]^{2-}$ is a poorer electron-donating ligand (or a better electron-withdrawing ligand) than $[\eta^5\text{-}Et_2C_2B_4H_4]^{2-}$.

Synthesis and Structure of 13-Vertex Cobaltacarborane (η^5-Cp)Co(η^6-$C_2B_{10}Me_8Et_2H_2$). Because the alkylation of the cage CH vertices in **3** and **4** was unsuccessful, we then turned to the cage carbon-substituted starting material in attempt to get additional information on the migration of two BH vertices. Compound 1,2-Et_2-4,5,7,8,9,10,11,12-Me_8-1,2-$C_2B_{10}H_2$ (**9**) was readily synthesized in 87% yield from the reaction of $Li_2C_2B_{10}Me_8H_2$ with 2 equiv of EtBr. Reduction of **9** with excess sodium metal followed by capitation reaction with $CoCl_2$/NaCp and aerobic oxidation gave, after column chromatographic separation, 4-Cp-1,9-Et_2-3,5,6,7,8,11,12,13-Me_8-4,1,9-$CoC_2B_{10}Me_8H_4$ (**10**) in 16% yield (Scheme 4). No other isomer was isolated from the reaction mixture. Complex **10** is thermally stable even in refluxing toluene, probably for the steric reasons. It is highly soluble in toluene, CH_2Cl_2, diethyl ether, and THF. The ^{1}H NMR spectrum of **10** showed a singlet of area 5 at 4.83 ppm assignable to the Cp protons, eight broad singlets of total area 24 at +0.7 to −0.3 ppm attributable to BMe protons, and two triplets of total area 6 corresponding to the methyl protons of the CH_2CH_3 groups, and four multiplets of the four methylene protons of the ethyl groups in the range 2.56 to 1.75 ppm. These data indicate the restricted rotation around the Et−C(cage) bonds in **10**. Its ^{11}B NMR spectrum displayed a 1:1:1:2:1:2:1:1 pattern in the range +31 to ∼−6 ppm. X-ray analyses confirmed that the cobalt atom, two C−Et vertices, and two BH vertices hold the 4, 1, 9, 2, and 10 positions,

---

(11) Yao, H.; Grimes, R. N. *Organometallics* **2003**, *22*, 4539.

respectively, leading to a docosahedral geometry (Figure 9). As indicated in Table 1, the structural parameters in **10** are very close to those observed in the above cobaltacarboranes. The two BH vertices are located on the hexagonal belt to minimize steric congestion. Such a very crowded environment may restrict the rotation of the Et−C(cage) bonds and limit the migration of the vertices, resulting in the formation of the thermodynamic product.

Alkyl-substituted carboranes **1** and **9** provide a means of detecting both carbon and boron atom rearrangements in 13-vertex metallacarboranes. The results show that the framework isomerization is substituent-dependent. All isomers produced can be rationalized by the DSD mechanism,[2g] as shown in Scheme 5. After careful examination, we find the equivalence between DSD and the rotation of pentagonal pyramidals in the docosahedron. Therefore, only rotation is indicated in Scheme 5 to simplify the drawings. According to this proposed mechanism, interconversion among all isolated metallacarboranes would be feasible, which is inconsistent with the experimental data showing no interconversion between **3** and **4** in refluxing THF. To account for this discrepancy, it is anticipated that a change of the substituents or a change of the isomers would influence the energies and lifetimes of the various possible intermediates, leading to the isolation of certain products under the specified reaction conditions.

Conclusion

This work shows that the reduction of *o*-$C_2B_{10}Me_8H_4$ with sodium or potassium metal gives *nido*-carborane dianion, in which the four unsubstituted vertices are all located on the hexagonal C_2B_4 open face. It is a kinetic product and isomerizes into a mixture of isomers upon heating. Capitation reaction of the *nido*-salt with $CoCl_2$/CpNa, followed by oxidation, affords two 13-vertex cobaltacarboranes: one contains the identical *nido*-carboranyl with that of the parent *nido*-salt, and the other bears its structural isomer with one BH vertex on the pentagonal belt. Upon heating, each of them can isomerize into a thermodynamically more stable one via the migration of the CH and/or BH vertex. More sterically demanding *o*-$C_2B_{10}Me_8Et_2H_2$ generates only one thermodynamically stable product via similar cage-opening and metal-insertion methodology. The results reveal that the steric factor plays a crucial role in the isomerization processes, and it is relatively easier to predict the positions of the two cage carbon vertices than those of two unsubstituted BH ones. All isomers can be rationalized via the popular DSD mechanism.

Nucleophilic substitution on the Cp ring of the mixed sandwich metallacarboranes is a very useful method for direct alkylation of the Cp ring in metallacarboranes of the C_2B_{10} systems. This research also shows that the C_2B_{10} ligands are poorer electron donors than the C_2B_4 ones.

Experimental Section

General Procedures. All experiments were performed under an atmosphere of dry dinitrogen with the rigid exclusion of air and moisture using standard Schlenk or cannula techniques or in a glovebox. All organic solvents were freshly distilled from sodium benzophenone ketyl immediately prior to use. 4,5,7,8,9,10,11,12-Me_8-1,2-$C_2B_{10}H_4$ (**1**) was prepared according to the literature method.[5] All other chemicals were purchased from either Aldrich or Acros Chemical Co. and used as received unless otherwise noted. IR spectra were obtained from KBr pellets prepared in the glovebox on a Perkin-Elmer 1600 Fourier transform spectrometer. ^1H and ^{13}C NMR spectra were recorded on a Bruker DPX 300 spectrometer at 300.13 and 75.47 MHz, respectively. ^{11}B NMR spectra were recorded on a Varian Inova 400 spectrometer at 128.32 MHz. All chemical shifts were reported in δ units with references to the residual solvent resonances of the deuterated solvents for ^1H and ^{13}C NMR chemical shifts and to external $BF_3{\cdot}OEt_2$ (0.00 ppm) for ^{11}B NMR chemical shifts. Mass spectra were recorded on a Thermo Finnigan MAT 95 XL spectrometer. Elemental analyses were performed by MEDAC Ltd., Middlesex, U.K.

Preparation of $\{[K(18\text{-crown-6})(THF)_2][K(18\text{-crown-6})]\}\{[4\text{-}(18\text{-crown-6})\text{-}2,3,5,8,9,11,12,13\text{-}Me_8\text{-}4,1,6\text{-}KC_2B_{10}H_4]_2\}$ (2). To a THF (25 mL) solution of **1** (0.26 g, 1.00 mmol) was added finely cut potassium metal (0.12 g, 3.00 mmol), and the mixture was stirred at room temperature for 3 days. After removal of excess potassium, a THF (10 mL) solution of 18-crown-6 (0.53 g, 2.00 mmol) was added to the resulting clear pale-yellow solution. The mixture was stirred at room temperature for 4 h and then concentrated to about 5 mL, to which was added toluene (∼5 mL). Complex **2** was isolated as colorless crystals after this solution stood at −30 °C for 2 days (0.73 g, 78%). ^1H NMR (pyridine-d_5): δ 3.64 (m, 4H, THF), 3.50 (m, 48H, 18-crown-6), 1.66 (m, 4H, THF), 1.30−0.00 (br, BCH_3). $^{13}C\{^1H\}$ NMR (pyridine-d_5): δ 69.49 (18-crown-6), 66.79, 24.78 (THF), −0.20 (br, BCH_3); the cage carbons were not observed. ^{11}B NMR (pyridine-d_5): δ 21.3 (1B, BCH_3), 20.3 (1B, BCH_3), 14.1 (1B, BCH_3), 6.9 (1B, BCH_3), −2.5 (1B, BCH_3), −3.7 (1B, BCH_3), −13.8 (1B, BCH_3), −16.8 (1B, $J_{B-H} = 131$ Hz, *B*H), −17.2 (1B, BCH_3), −19.5 (1B, $J_{B-H} = 130$ Hz, *B*H). IR (KBr, cm^{-1}): ν_{BH} 2379 (w), 2324 (w). Anal. Calcd for $C_{38}H_{82}B_{10}K_2O_{13}$ (**2**): C, 48.90; H, 6.32. Found: C, 48.61; H, 6.08.

Preparation of 4-Cp-2,3,5,8,9,11,12,13-Me_8-4,1,6-$CoC_2B_{10}Me_8H_4$ (3) and 4-Cp-2,3,5,9,10,11,12,13-Me_8-4,1,6-$CoC_2B_{10}Me_8H_4$ (4). To a THF (100 mL) solution of **1** (2.56 g, 10.0 mmol) was added finely cut sodium metal (0.69 g, 30.0 mmol), and the mixture was stirred at room temperature for 3 days. After removal of excess sodium metal, NaCp (2.64 g, 30.0 mmol) was added to give a pink solution. At −78 °C, the resulting solution was transferred into a THF (30 mL) suspension of $CoCl_2$ (5.20 g, 40.0 mmol), and the mixture was stirred at room temperature for 2 days to yield a deep-brown suspension. A stream of oxygen was passed through this suspension for 1 h. The reaction mixture was then filtered through Celite, and the residue was washed with CH_2Cl_2 until it turned to pale yellow. The organic solutions were combined and concentrated to yield a brown solid. Chromatographic separation (SiO_2, 300−400 mesh, hexane/dichloromethane (8:1) as the eluant) afforded **3** (0.57 g, 15%) and **4** (0.30 g, 8%) both as a deep-red solid. Single crystals suitable for X-ray analyses were obtained from the hexane solution. For **3**. ^1H NMR ($CDCl_3$): δ 5.21 (s, 5H, C_5H_5), 4.14 (s, 1H, cage C*H*), 3.03 (s, 1H, cage C*H*), 0.94 (s, 3H, BCH_3), 0.33 (s, 3H, BCH_3), 0.16 (s, 6H, BCH_3), 0.07 (s, 3H, BCH_3), 0.01 (s, 3H, BCH_3), −0.39 (s, 3H, BCH_3), −0.59 (s, 3H, BCH_3). $^{13}C\{^1H\}$ NMR ($CDCl_3$): δ 88.78 (C_5H_4), 9.02 (br, BCH_3), 2.07 (br, BCH_3); the cage carbons were not observed. ^{11}B NMR ($CDCl_3$): δ 15.6 (1B, BCH_3), 14.5 (1B, $J_{B-H} = 120$ Hz, *B*H), 13.5 (1B, BCH_3), 5.3 (2B, BCH_3), 0.63 (2B, BCH_3), −4.1 (1B, BCH_3), −5.0 (1B, $J_{B-H} = 132$ Hz, *B*H), −6.2 (1B, BCH_3). IR (KBr, cm^{-1}): ν_{BH} 2497 (m), 2334 (w). HRMS. Calcd for $C_{15}H_{33}{}^{11}B_8{}^{10}B_2Co^+$: *m*/*z* 380.2913. Found:

m/*z* 380.2917. For **4**. ^{1}H NMR ($\mathrm{CDCl_3}$): δ 5.16 (s, 5H, C_5H_5), 3.88 (s, 1H, cage $\mathrm{C}H$), 3.17 (s, 1H, cage $\mathrm{C}H$), 0.94 (s, 3H, $\mathrm{BC}H_3$), 0.39 (s, 3H, $\mathrm{BC}H_3$), 0.26 (s, 3H, $\mathrm{BC}H_3$), 0.20 (s, 3H, $\mathrm{BC}H_3$), 0.16 (s, 3H, $\mathrm{BC}H_3$), −0.24 (s, 3H, $\mathrm{BC}H_3$), −0.34 (s, 3H, $\mathrm{BC}H_3$), −0.45 (s, 3H, $\mathrm{BC}H_3$). ^{13}C{^{1}H} NMR ($\mathrm{CDCl_3}$): δ 88.90 ($C_5\mathrm{H}_4$), 8.52 (br, $\mathrm{B}C\mathrm{H}_3$), 2.40 (br, $\mathrm{B}C\mathrm{H}_3$); the cage carbons were not observed. ^{11}B NMR ($\mathrm{CDCl_3}$): δ 13.0 (2B, $B\mathrm{CH}_3$ + BH (overlapped)), 10.8 (1B, $B\mathrm{CH}_3$), 5.0 (2B, $B\mathrm{CH}_3$), 0.6 (1B, $B\mathrm{CH}_3$), −1.6 (1B, $J_{\mathrm{B-H}} = 120$ Hz, BH), −2.7 (1B, $B\mathrm{CH}_3$), −4.1 (1B, $B\mathrm{CH}_3$), −8.3 (1B, $B\mathrm{CH}_3$). IR (KBr, cm^{-1}): ν_{BH} 2479 (m). HRMS. Calcd for $\mathrm{C_{15}H_{33}{}^{11}B_8{}^{10}B_2Co^+}$: *m*/*z* 380.2913. Found: *m*/*z* 380.2911.

Preparation of 4-Cp-2,3,5,6,8,11,12,13-Me$_8$-4,1,9-CoC$_2$B$_{10}$Me$_8$H$_4$ (5). A THF (10 mL) solution of **3** (0.19 g, 0.50 mmol) was heated to reflux for 12 h. The color of the solution turned from red-brown to red. After cooling to room temperature and removal of THF, column chromatographic separation ($\mathrm{SiO_2}$, 300−400 mesh, hexane/dichloromethane (8:1) as the eluant) gave **5** as red crystals (0.17 g, 90%). ^{1}H NMR ($\mathrm{CDCl_3}$): δ 4.95 (s, 5H, C_5H_5), 3.54 (s, 1H, cage $\mathrm{C}H$), 1.53 (s, 1H, cage $\mathrm{C}H$), 0.81 (s, 3H, $\mathrm{BC}H_3$), 0.70 (s, 3H, $\mathrm{BC}H_3$), 0.58 (s, 3H, $\mathrm{BC}H_3$), 0.18 (s, 3H, $\mathrm{BC}H_3$), 0.09 (s, 3H, $\mathrm{BC}H_3$), 0.01 (s, 3H, $\mathrm{BC}H_3$), −0.16 (s, 3H, $\mathrm{BC}H_3$), −0.27 (s, 3H, $\mathrm{BC}H_3$). ^{13}C{^{1}H} NMR ($\mathrm{CDCl_3}$): δ 89.2 ($C_5\mathrm{H}_4$), 11.1 (br, $\mathrm{B}C\mathrm{H}_3$), 2.7 (br, $\mathrm{B}C\mathrm{H}_3$); the cage carbons were not observed. ^{11}B NMR ($\mathrm{CDCl_3}$): δ 23.2 (1B, $J_{\mathrm{B-H}} = 128$ Hz, BH), 17.1 (1B, $B\mathrm{CH}_3$), 13.0 (1B, $B\mathrm{CH}_3$), 9.1 (1B, $J_{\mathrm{B-H}} = 134$ Hz, BH), 6.6 (1B, $B\mathrm{CH}_3$), 5.8 (1B, $B\mathrm{CH}_3$), 3.2 (2B, $B\mathrm{CH}_3$), 1.2 (1B, $B\mathrm{CH}_3$), −4.7 (1B, $B\mathrm{CH}_3$). IR (KBr, cm^{-1}): ν_{BH} 2476 (m), 2334 (w). HRMS. Calcd for $\mathrm{C_{15}H_{33}{}^{11}B_8{}^{10}B_2Co^+}$: *m*/*z* 380.2913. Found: *m*/*z* 380.2917.

Preparation of 4-Cp-2,3,5,6,7,11,12,13-Me$_8$-4,1,9-CoC$_2$B$_{10}$Me$_8$H$_4$ (6). A THF (10 mL) solution of **4** (0.19 g, 0.50 mmol) was heated to reflux for 12 h. The color of the solution turned from red-brown to red. After cooling to room temperature and removal of THF, column chromatographic separation ($\mathrm{SiO_2}$, 300−400 mesh, hexane/dichloromethane (8:1) as the eluant) gave **6** as red crystals (0.17 g, 90%). ^{1}H NMR ($\mathrm{CDCl_3}$): δ 4.83 (s, 5H, C_5H_5), 3.61 (s, 1H, cage $\mathrm{C}H$), 1.44 (s, 1H, cage $\mathrm{C}H$), 0.76 (s, 3H, $\mathrm{BC}H_3$), 0.70 (s, 3H, $\mathrm{BC}H_3$), 0.65 (s, 3H, $\mathrm{BC}H_3$), 0.51 (s, 3H, $\mathrm{BC}H_3$), 0.19 (s, 3H, $\mathrm{BC}H_3$), 0.15 (s, 3H, $\mathrm{BC}H_3$), −0.02 (s, 3H, $\mathrm{BC}H_3$), −0.14 (s, 3H, $\mathrm{BC}H_3$). ^{13}C{^{1}H} NMR ($\mathrm{CDCl_3}$): δ 89.9 ($C_5\mathrm{H}_4$), 11.2 (br, $\mathrm{B}C\mathrm{H}_3$), 1.1 (br, $\mathrm{B}C\mathrm{H}_3$); the cage carbons were not observed. ^{11}B NMR ($\mathrm{CDCl_3}$): δ 28.6 (1B, $B\mathrm{CH}_3$), 14.1 (1B, $B\mathrm{CH}_3$), 11.5 (1B, $B\mathrm{CH}_3$), 9.7 (1B, $J_{\mathrm{B-H}} = 128$ Hz, BH), 3.8 (2B, $B\mathrm{CH}_3$), 0.9 (3B, $B\mathrm{CH}_3$), −9.9 (1B, $J_{\mathrm{B-H}} = 130$ Hz, BH). IR (KBr, cm^{-1}): ν_{BH} 2481 (m), 2334 (m). HRMS. Calcd for $\mathrm{C_{15}H_{33}{}^{11}B_8{}^{10}B_2Co^+}$: *m*/*z* 380.2913. Found: *m*/*z* 380.2918.

Preparation of 4-^{n}BuCp-2,3,5,8,9,11,12,13-Me$_8$-4,1,6-CoC$_2$B$_{10}$Me$_8$H$_4$ (7). To a THF (10 mL) solution of **3** (0.19 g, 0.50 mmol) was added ^{n}BuLi (0.31 mL, 1.6 M in hexane, 0.50 mmol) at −78 °C. The mixture was then stirred at room temperature for 1 h, giving a deep-red solution. After removal of the solvent, the residue was subjected to column chromatographic separation ($\mathrm{SiO_2}$, 300−400 mesh, hexane/dichloromethane (8:1) as the eluant), affording **7** as red crystals (0.16 g, 82%). ^{1}H NMR ($\mathrm{CDCl_3}$): δ 5.26 (brs, 1H, $^n\mathrm{BuC}_5H_4$), 5.04 (brs, 1H, $^n\mathrm{BuC}_5H_4$), 4.97 (brs, $^n\mathrm{BuC}_5H_4$), 4.84 (brs, 1H, $^n\mathrm{BuC}_5H_4$), 3.90 (s, 1H, cage $\mathrm{C}H$), 2.73 (s, 1H, cage $\mathrm{C}H$), 2.27 (m, 2H, $\mathrm{C}H_2\mathrm{CH_2CH_2CH_3}$), 1.48 (m, 2H, $\mathrm{CH_2C}H_2\mathrm{CH_2CH_3}$), 1.33 (m, 2H, $\mathrm{CH_2CH_2C}H_2\mathrm{CH_3}$), 0.93 (s, 3H, $\mathrm{BC}H_3$), 0.90 (t, J = 3.0 Hz, 3H, $\mathrm{CH_2CH_2CH_2C}H_3$), 0.31 (s, 3H, $\mathrm{BC}H_3$), 0.15 (s, 6H, $\mathrm{BC}H_3$), 0.08 (s, 3H, $\mathrm{BC}H_3$), 0.00 (s, 3H, $\mathrm{BC}H_3$), −0.40 (s, 3H, $\mathrm{BC}H_3$), −0.61 (s, 3H, $\mathrm{BC}H_3$). ^{13}C{^{1}H} NMR ($\mathrm{CDCl_3}$): δ 110.0, 89.7, 88.5, 87.9, 87.7 ($^n\mathrm{Bu}C_5\mathrm{H}_4$), 32.3, 27.0, 22.3, 13.7 (^{n}Bu), 9.9 (br, $\mathrm{B}C\mathrm{H}_3$), 2.5 (br, $\mathrm{B}C\mathrm{H}_3$); the cage carbons were not observed. ^{11}B NMR ($\mathrm{CDCl_3}$): δ 15.4 (1B, $B\mathrm{CH}_3$), 13.9 (1B, $J_{\mathrm{B-H}} = 149$ Hz, BH), 12.6 (1B, $B\mathrm{CH}_3$), 5.0 (2B, $B\mathrm{CH}_3$), 0.2 (2B, $B\mathrm{CH}_3$), −4.5 (2B, $B\mathrm{CH}_3$ + BH (overlapped)), −6.6 (1B, $B\mathrm{CH}_3$). IR (KBr, cm^{-1}): ν_{BH} 2490 (m), 2283 (m). HRMS. Calcd for $\mathrm{C_{19}H_{41}{}^{11}B_8{}^{10}B_2Co^+}$: *m*/*z* 436.3539. Found: *m*/*z* 436.3551.

Preparation of 4-^{n}BuCp-2,3,5,9,10,11,12,13-Me$_8$-4,1,6-CoC$_2$B$_{10}$Me$_8$H$_4$ (8a). This complex was prepared as deep-red crystals (0.17 g, 85%) from the reaction of **4** (0.19 g, 0.50 mmol) with ^{n}BuLi (0.31 mL, 1.6 M in hexane, 0.50 mmol) in THF (10 mL) using the same procedure as that for **7**. ^{1}H NMR ($\mathrm{CDCl_3}$): δ 5.20 (brs, 1H, $^n\mathrm{BuC}_5H_4$), 5.02 (brs, 2H, $^n\mathrm{BuC}_5H_4$), 4.81 (brs, 1H, $^n\mathrm{BuC}_5H_4$), 3.51 (s, 1H, cage $\mathrm{C}H$), 2.88 (s, 1H, cage $\mathrm{C}H$), 2.38 (m, 2H, $\mathrm{C}H_2\mathrm{CH_2CH_2CH_3}$), 1.52 (m, 2H, $\mathrm{CH_2C}H_2\mathrm{CH_2CH_3}$), 1.33 (m, 2H, $\mathrm{CH_2CH_2C}H_2\mathrm{CH_3}$), 0.94 (t, J = 6.0 Hz, 3H, $\mathrm{CH_2CH_2CH_2C}H_3$), 0.89 (s, 3H, $\mathrm{BC}H_3$), 0.38 (s, 3H, $\mathrm{BC}H_3$), 0.26 (s, 6H, $\mathrm{BC}H_3$), 0.19 (s, 3H, $\mathrm{BC}H_3$), −0.15 (s, 3H, $\mathrm{BC}H_3$), −0.25 (s, 3H, $\mathrm{BC}H_3$), −0.36 (s, 3H, $\mathrm{BC}H_3$). ^{13}C{^{1}H} NMR ($\mathrm{CDCl_3}$): δ 110.5, 88.9, 88.1, 87.4, 87.0 ($^n\mathrm{Bu}C_5\mathrm{H}_4$), 32.0, 27.5, 22.2, 13.8 (^{n}Bu), 8.7 (br, $\mathrm{B}C\mathrm{H}_3$), 2.5 (br, $\mathrm{B}C\mathrm{H}_3$); the cage carbons were not observed. ^{11}B NMR ($\mathrm{CDCl_3}$): δ 13.5 (2B, $B\mathrm{CH}_3$), 12.7 (1B, $J_{\mathrm{B-H}} = 126$ Hz, BH), 5.8 (2B, $B\mathrm{CH}_3$), 1.7 (1B, $B\mathrm{CH}_3$), 0.1 (1B, $J_{\mathrm{B-H}} = 139$ Hz, BH), −2.3 (1B, $B\mathrm{CH}_3$), −3.2 (1B, $B\mathrm{CH}_3$). −7.0 (1B, $B\mathrm{CH}_3$). IR (KBr, cm^{-1}): ν_{BH} 2478 (m), 2341 (m). HRMS. Calcd for $\mathrm{C_{19}H_{41}{}^{11}B_8{}^{10}B_2Co^+}$: *m*/*z* 436.3539. Found: *m*/*z* 436.3539.

Preparation of 4-MeCp-2,3,5,9,10,11,12,13-Me$_8$-4,1,6-CoC$_2$B$_{10}$Me$_8$H$_4$ (8b). This complex was prepared as deep-red crystals (0.17 g, 85%) from the reaction of **4** (0.19 g, 0.50 mmol) with MeLi (0.31 mL, 1.6 M in hexane, 0.50 mmol) in THF (10 mL) using the same procedure as that for **7**. ^{1}H NMR ($\mathrm{CDCl_3}$): δ 5.30 (brs, 1H, MeC_5H_4), 5.19 (brs, 1H, MeC_5H_4), 4.88 (brs, 1H, MeC_5H_4), 4.81 (brs, 1H, MeC_5H_4), 2.88 (s, 1H, cage $\mathrm{C}H$), 2.04 (s, 3H, $\mathrm{CpC}H_3$), 1.56 (s, 1H, cage $\mathrm{C}H$), 0.90 (s, 3H, $\mathrm{BC}H_3$), 0.39 (s, 3H, $\mathrm{BC}H_3$), 0.26 (s, 3H, $\mathrm{BC}H_3$), 0.19 (s, 3H, $\mathrm{BC}H_3$), 0.16 (s, 3H, $\mathrm{BC}H_3$), −0.15 (s, 3H, $\mathrm{BC}H_3$), −0.24 (s, 3H, $\mathrm{BC}H_3$), −0.35 (s, 3H, $\mathrm{BC}H_3$). ^{13}C{^{1}H} NMR ($\mathrm{CDCl_3}$): δ 106.1, 90.4, 89.9, 89.1, 87.9 ($\mathrm{Me}C_5\mathrm{H}_4$), 12.9 ($\mathrm{Cp}C\mathrm{H}_3$), 8.9 (br, $\mathrm{B}C\mathrm{H}_3$), 2.2 (br, $\mathrm{B}C\mathrm{H}_3$); the cage carbons were not observed. ^{11}B NMR ($\mathrm{CDCl_3}$): δ 12.0 (2B, $B\mathrm{CH}_3$), 11.0 (1B, $J_{\mathrm{B-H}} = 126$ Hz, BH), 4.2 (2B, $B\mathrm{CH}_3$), 0.2 (1B, $B\mathrm{CH}_3$), −1.4 (1B, $J_{\mathrm{B-H}} = 139$ Hz, BH), −3.8 (1B, $B\mathrm{CH}_3$), −4.8 (1B, $B\mathrm{CH}_3$), −8.5 (1B, $B\mathrm{CH}_3$). IR (KBr, cm^{-1}): ν_{BH} 2474 (s). HRMS. Calcd for $\mathrm{C_{16}H_{35}{}^{11}B_8{}^{10}B_2Co^+}$: *m*/*z* 396.2996. Found: *m*/*z* 396.3008.

Preparation of 1,2-Et$_2$-4,5,7,8,9,10,11,12-Me$_8$-1,2-C$_2$B$_{10}$H$_2$ (9). A diethyl ether solution (20 mL) of **1** (0.51 g, 2.00 mmol) was treated with ^{n}BuLi (2.50 mL, 1.6 M in hexane, 4.00 mmol) at 0 °C. The mixture was stirred at room temperature for 1 day, giving a pale-yellow solution, to which was added EtBr (0.24 g, 2.20 mmol) at −78 °C. The mixture was then stirred at room temperature for 8 h. After quenching with a saturated $\mathrm{NaHCO_3}$ aqueous solution, the organic layer was separated, and the aqueous layer was extracted with $\mathrm{Et_2O}$ (20 mL × 3). The combined organic portions were dried over anhydrous $\mathrm{Na_2SO_4}$. After removal of $\mathrm{Na_2SO_4}$ and the solvent, the resultant solid was subjected to chromatographic separation ($\mathrm{SiO_2}$, 300−400 mesh) using hexane as the eluant to give **9** as a white powder (0.54 g, 87%). ^{1}H NMR ($\mathrm{CDCl_3}$): δ 2.26 (q, J = 6.0 Hz, 4H, $\mathrm{C}H_2\mathrm{CH_3}$), 1.08 (t, J = 6.0 Hz, 6H, $\mathrm{CH_2C}H_3$), 0.07 (s, 3H, $\mathrm{BC}H_3$), 0.70 (br, 12H, $\mathrm{BC}H_3$), −0.06 (br, 6H, $\mathrm{BC}H_3$), −0.42 (br, 6H, $\mathrm{BC}H_3$). ^{13}C{^{1}H} NMR ($\mathrm{CDCl_3}$): δ 25.1 ($C\mathrm{H_2CH_3}$), 13.0 ($\mathrm{CH_2}C\mathrm{H_3}$), −3.6 (br, $\mathrm{B}C\mathrm{H}_3$). ^{11}B NMR ($\mathrm{CDCl_3}$): δ 5.1 (2B, $B\mathrm{CH}_3$), −3.6 (2B, $B\mathrm{CH}_3$), −6.6 (4B, $B\mathrm{CH}_3$), −13.0 (2B, $J_{\mathrm{B-H}} = 169$ Hz, BH). IR (KBr, cm^{-1}): ν_{BH} 2450 (m). HRMS. Calcd for $\mathrm{C_{14}H_{36}{}^{11}B_8{}^{10}B_2{}^+}$: *m*/*z* 312.3816. Found: *m*/*z* 312.3817.

Preparation of 4-Cp-1,9-Et$_2$-2,5,6,7,8,11,12,13-Me$_8$-4,1,9-CoC$_2$B$_{10}$Me$_8$H$_4$ (10). This complex was prepared as red crystals from **9** (0.62 g, 2.00 mmol), sodium metal (0.10 g, 4.00 mmol), NaCp (0.53 g, 6.00 mmol), and $CoCl_2$ (1.04 g, 8.00 mmol) using the same procedure as that described for **4**. Yield: 0.14 g (16%). ^{1}H NMR ($CDCl_3$): δ 4.83 (s, 5H, C_5H_5), 2.56 (m, 1H, CH_2CH_3), 2.30 (m, 1H, CH_2CH_3), 2.00 (m, 1H, CH_2CH_3), 1.75 (m, 1H, CH_2CH_3), 1.38 (t, $J = 9.0$ Hz, 3H, CH_2CH_3), 0.91 (t, $J = 9.0$ Hz, 3H, CH_2CH_3), 0.66 (s, 3H, BCH_3), 0.61 (s, 3H, BCH_3), 0.32 (s, 3H, BCH_3), −0.01 (s, 3H, BCH_3), −0.07 (s, 3H, BCH_3), −0.18 (s, 3H, BCH_3), −0.25 (s, 3H, BCH_3), −0.30 (s, 3H, BCH_3). ^{13}C{^{1}H} NMR ($CDCl_3$): δ 90.7 (C_5H_4), 33.0 (CH_2CH_3), 28.7 (CH_2CH_3), 21.0 (CH_2CH_3), 13.7 (CH_2CH_3), 5.5 (br, BCH_3), 1.2 (br, BCH_3); the cage carbons were not observed. ^{11}B NMR ($CDCl_3$): δ 30.5 (1B, BCH_3), 16.0 (1B, BCH_3), 13.4 (1B, BCH_3), 7.8 (2B, BCH_3, BH), 5.1 (1B, BCH_3), 3.0 (2B, BCH_3), −0.6 (1B, $J_{B-H} = 145$ Hz, BH), −5.2 (1B, BCH_3). IR (KBr, cm^{-1}): ν_{BH} 2446 (m), 2300 (m). HRMS. Calcd for $C_{19}H_{41}{}^{11}B_8{}^{10}B_2Co^+$: m/z 436.3539. Found: m/z 436.3546.

X-ray Structure Determination. Data were collected at 293 K on a Bruker SMART 1000 CCD diffractometer using Mo Kα radiation. An empirical absorption correction was applied using the *SADABS* program.[12] All structures were solved by direct methods and subsequent Fourier difference techniques and refined anisotropically for all non-hydrogen atoms by full-matrix least-squares calculations on F^2 using the *SHELXTL* program package.[13] All hydrogen atoms were geometrically fixed using the riding model. Crystal data and details of data collection and structure refinements are given in Tables 2 and 3. Selected bond distances and angles are compiled in Table 1. It is noted that C8/B9 atoms of the cage in **6** and C6/B7 atoms of the cage in **8b** are indistinguishable because of the presence of a crystallographic mirror plane passing through the Co4, C1, and B10 atoms (Figures 5 and 8). Therefore, the independent carbon atoms in **6** and **8b** are assigned the site occupancy factor (SOF) of 0.917, which is calculated from the equation $(6 + 5)/(6 + 6)$, and the C19 atom in **8b** is assigned the SOF of 0.5. Further details are included in the Supporting Information.

Acknowledgment. The work described in this paper was supported by grants from the Research Grants Council of The Hong Kong Special Administration Region (Project 403906) and a Strategic Investments Scheme administrated by The Chinese University of Hong Kong.

Supporting Information Available: X-ray crystallographic files in CIF format for complexes **2**−**7**, **8a**, **8b**, and **10**. This material is available free of charge via the Internet at http://pubs.acs.org.

IC062423T

---

(12) Sheldrick, G. M. *SADABS: Program for Empirical Absorption Correction of Area Detector Data*; University of Göttingen: Göttingen, Germany, 1996.

(13) Sheldrick, G. M. *SHELXTL 5.10 for Windows NT: Structure Determination Software Programs*; Bruker Analytical X-ray Systems, Inc.: Madison, WI, 1997.